JOURNAL OF COMPUTATIONAL PHYSICS 98, 90–100 (1992)

A Formula for Estimation of Truncation Errors of Convection Terms in a Curvilinear Coordinate System

D. LEE AND Y. M. TSUEI

Institute of Aeronautics and Astronautics, National Cheng Kung University, Tainan, Taiwan, Republic of China

Received February 23, 1990; revised December 18, 1990

A formula for truncation errors of convection terms arising from the Navier–Stokes equation in a curvilinear coordinate system is derived. These truncation error terms are interpreted in terms of grid size, grid uniformity, grid line angle, flow angle, and derivatives of flow properties to gain physical insights from the formula. The role of these factors in determining truncation errors is discussed. It is shown that an optimal grid arrangement cannot be obtained without considering the interactions between the grid and the flow field. The effect of the grid orthogonality on truncation errors is also analyzed for simple cases. The derived formula provides a useful indicator for truncation error distribution which yields guidelines for grid adaption.

INTRODUCTION

Body-fitted coordinate system is becoming more widely employed in Navier–Stokes equation solvers due to its flexibility in handling complex geometry and in utilizing grid generation techniques. In transforming to a general curvilinear coordinate, the governing equations become more complicated and there is ambiguity in the analysis of truncation errors after transformation. de Rivas [1] concluded that grid nonuniformity increased truncation errors. Castro and Jones [2] also found that nonuniformity may lower the order of the truncation errors. Forester [3] suggested that grid size ratio between two neighboring grids should be kept under two. A more detailed study on this subject was conducted by Thompson and Mastin [4] and Thompson *et al.* [5]. In these two studies, the leading truncation error term for a first derivative is derived and the authors concluded that if the angle between grid lines is no less than 45°, the errors attributed to grid nonorthogonality are of little concern. In the present study, an effort is made to clarify the role of each factor described above. A formula for the truncation errors of two-dimensional convection terms in a curvilinear coordinate system is derived. The expression obtained is interpreted in terms of grid size, grid size ratio, angle between grid lines, and derivatives of flow properties to gain physical insights. Useful guidelines for grid distributing can be derived from these truncation error expressions. By using the derived formula as an error indicator, an adaptive grid method is employed to illustrate that with appropriate grid adaption the truncation error can be reduced.

TRUNCATION ERRORS OF TWO-DIMENSIONAL CONVECTION TERMS

The derivation starts from the truncation error of the first derivative term. Following the analysis of Thompson *et al.* [5] and using the second-order upwind differencing scheme, the first derivative term f_x can be expressed as

$$f_x = \frac{1}{J}\left[y_\eta \frac{-3f_{i,j} + 4f_{i+1,j} - f_{i+2,j}}{2\,\Delta\xi} - y_\xi \frac{-3f_{i,j} + 4f_{i,j+1} - f_{i,j+2}}{2\,\Delta\eta}\right] + T_x, \tag{1}$$

where $J \equiv x_\xi y_\eta - x_\eta y_\xi$ is the Jacobian, ξ, η are the general coordinates, and the truncation error T_x is

$$T_x = \frac{1}{3J}\left[y_\eta f_{\xi\xi\xi}\,\Delta\xi^2 - y_\xi f_{\eta\eta\eta}\,\Delta\eta^2\right] + \text{Higher Order Terms.} \tag{2}$$

Up to this stage, the metric coefficients and the Jacobian J are kept in their exact form. If $f_{\xi\xi\xi}, f_{\eta\eta\eta}$ are further expanded by using total differentiation, T_x can be expressed as

$$T_x = T_{x1} + T_{x2} + T_{x3} + \text{Higher Order Terms}, \tag{3}$$

where T_{x1} is the truncation error which contains the first derivatives of f, T_{x2} the second derivatives, and T_{x3} the third derivatives. That is, by taking $\Delta\xi = \Delta\eta = 1$,

$$T_{x1} = \frac{1}{3J}\left[(y_\eta x_{\xi\xi\xi} - y_\xi x_{\eta\eta\eta})\, f_x + (y_\eta y_{\xi\xi\xi} - y_\xi y_{\eta\eta\eta})\, f_y\right] \tag{4}$$

0021-9991/92 $3.00

$$T_{x2}=\frac{1}{J}[(x_\xi y_\eta x_{\xi\xi}-x_\eta y_\xi x_{\eta\eta})f_{xx}$$
$$+(y_\xi y_\eta x_{\xi\xi}+x_\xi y_\eta y_{\xi\xi}-y_\xi y_\eta x_{\eta\eta}-x_\eta y_\xi y_{\eta\eta})f_{xy}$$
$$+(y_\xi y_\eta y_{\xi\xi}-y_\xi y_\eta y_{\eta\eta})f_{yy}] \quad (5)$$

$$T_{x3}=\frac{1}{3J}[(y_\eta x_\xi^3-y_\xi x_\eta^3)f_{xxx}+3(y_\xi y_\eta x_\xi^2-y_\xi y_\eta x_\eta^2)f_{xxy}$$
$$+3(x_\xi y_\eta y_\xi^2-x_\eta y_\xi y_\eta^2)f_{xyy}+(y_\eta y_\xi^3-y_\xi y_\eta^3)f_{yyy}]. \quad (6)$$

If the metric coefficients are evaluated numerically by the same second-order upwind scheme used above, for example,

$$x_\xi=\frac{-x_{i,j}+4x_{i+1,j}-3x_{i+2,j}}{2\,\Delta\xi}+\frac{1}{3}x_{\xi\xi\xi}(\Delta\xi)^2$$
$$+\text{Higher Order Terms}$$

then by substituting these metric coefficients and J in Eq. (1), f_x becomes

$$f_x=\frac{1}{J+\Delta J}\left\{\left[y_\eta+\frac{1}{3}y_{\eta\eta\eta}(\Delta\eta)^2\right]\left[f_\xi+\frac{1}{3}f_{\xi\xi\xi}(\Delta\xi)^2\right]\right.$$
$$\left.-\left[y_\xi+\frac{1}{3}y_{\xi\xi\xi}(\Delta\xi)^2\right]\left[f_\eta+\frac{1}{3}f_{\eta\eta\eta}\right]\right\}$$
$$+\text{Higher Order Terms},$$

where

$$\Delta J=\tfrac{1}{3}[x_\xi y_{\eta\eta\eta}(\Delta\eta)^2+y_\eta x_{\xi\xi\xi}(\Delta\xi)^2-y_\xi x_{\eta\eta\eta}(\Delta\eta)^2$$
$$-x_\eta y_{\xi\xi\xi}(\Delta\xi)^2]+\text{Higher Order Terms}.$$

After similar manipulations, it is found that T_{x1} vanishes, and T_x becomes

$$T_x=T_{x2}+T_{x3}+\text{Higher Order Terms}. \quad (7)$$

Note that this is the same expression obtained by Thompson *et al.* [5] in one-dimensional form. However, if the metric coefficients are evaluated by the second-order central scheme, as they are in the present study, T_{x1} appears again with the same form as Eq. (4), except that the leading constant $\frac{1}{3}$ is replaced by $\frac{1}{2}$. T_{x2} and T_{x3} remain the same as in Eqs. (5) and (6).

For the two-dimensional convection terms written in the form

$$\rho u\frac{\partial f}{\partial x}+\rho v\frac{\partial f}{\partial y} \quad (8)$$

their transformed form is

$$\frac{1}{J}\left[\rho\bar{U}\frac{\partial f}{\partial\xi}+\rho\bar{V}\frac{\partial f}{\partial\eta}\right], \quad (9)$$

where $\bar{U}$, $\bar{V}$ are the contravariant velocities

$$\bar{U}=uy_\eta-vx_\eta$$
$$\bar{V}=vx_\xi-uy_\xi. \quad (10)$$

By using the second-order upwind differencing scheme for the convection terms and the second-order central scheme for the metric coefficients and substituting the truncation expression T_x and its counterpart for T_y into Eq. (8), one may obtain the truncation errors T_E for the convection terms of Eq. (8) as

$$T_E=\rho u(T_x)+\rho v(T_y)$$
$$=T_{E1}+T_{E2}+T_{E3}+\text{Higher Order Terms}, \quad (11)$$

where

$$T_{E1}=\frac{\rho}{2J}[(\bar{U}x_{\xi\xi\xi}+\bar{V}x_{\eta\eta\eta})f_x+(\bar{U}y_{\xi\xi\xi}+\bar{V}y_{\eta\eta\eta})f_y] \quad (12)$$

$$T_{E2}=\frac{\rho}{J}\{(\bar{U}x_\xi x_{\xi\xi}+\bar{V}x_\eta x_{\eta\eta})f_{xx}+[\bar{U}(y_\xi x_{\xi\xi}+x_\xi y_{\xi\xi})$$
$$+\bar{V}(y_\eta x_{\eta\eta}+x_\eta y_{\eta\eta})]f_{xy}+(\bar{U}y_\xi y_{\xi\xi}+\bar{V}y_\eta y_{\eta\eta})f_{yy}\} \quad (13)$$

$$T_{E3}=\frac{\rho}{3J}[(\bar{U}x_\xi^3+\bar{V}x_\eta^3)f_{xxx}+3(\bar{U}x_\xi^2y_\xi+\bar{V}x_\eta^2y_\eta)f_{xxy}$$
$$+3(\bar{U}x_\xi y_\xi^2+\bar{V}x_\eta y_\eta^2)f_{xyy}+(\bar{U}y_\xi^3+\bar{V}y_\eta^3)f_{yyy}]. \quad (14)$$

It is noted that T_{E1} appears since, as mentioned above, a scheme other than that used in Eq. (8) is employed for the metric coefficients. Equations (12) to (14) are the truncation errors for the two-dimensional convection terms up to third derivatives of f. The physical interpretation of Eqs. (12) to (14) is not clear in their present forms. To further interpret the meaning of these terms, one can substitute physical dimensions and angles between grid lines for those metric coefficients as detailed in the following.

Figure 1 shows the definitions and relationships among different angles and grid sizes. In the analysis, a and b are the grid sizes for the grid cell at $(\xi, \eta)=(i, j)$, θ is the angle between coordinate lines at (i, j), and β is the angle between the η line and the y axis, γ is the angle between the ξ line and the x axis, i.e., $\theta+\beta+\gamma=90°$; r_1, r_{11}, r_{12} are the grid size ratios relative to the grid size a in the ξ direction. On the

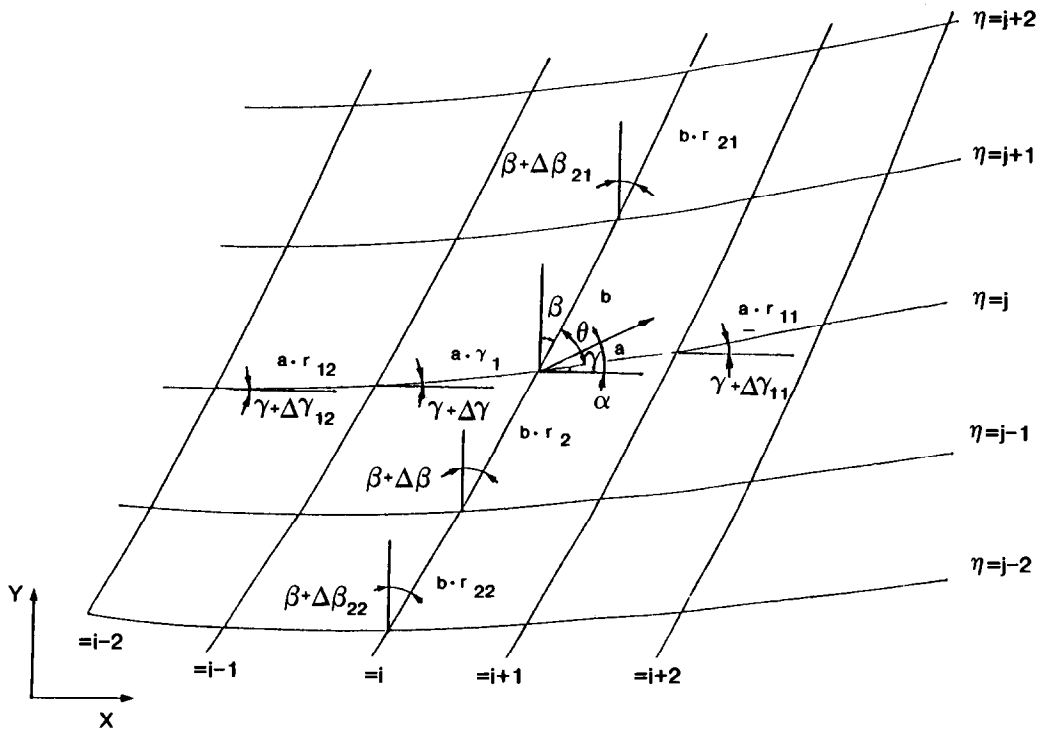

FIG. 1. Physical dimensions and angles in the formula.

other hand, r_2, r_{21}, r_{22} are those relative to the grid size b along the η direction. Note that for a uniform grid, the value of r is unity. $\Delta\beta$'s and $\Delta\gamma$'s are the changes of angles between neighboring grids. The metric coefficients in Eqs. (12) to (14) can be expressed in terms of these angles and grid size ratios, for example, with $\Delta\xi = \Delta\eta = 1$,

$$x_\xi = \frac{x_{i+1,j} - x_{i,j}}{\Delta\xi} = x_{i+1,j} - x_{i,j} = a\cos\gamma$$

and, similarly,

$$\begin{aligned} x_\eta &= b\sin\beta \\ y_\xi &= a\sin\gamma \\ y_\eta &= b\cos\beta \\ J &\equiv x_\xi y_\eta - x_\eta y_\xi = ab\sin\theta. \end{aligned} \tag{15}$$

Note that the one-sided differencing scheme is used here to insert the physical dimensions and grid angles into the truncation error formula. Higher order schemes can also be used but the resulting expressions will become much more complicated and harder to interpret. Moreover, in deriving the following expressions the main object is to show the relevant physical factors which compose the formula. For this purpose, the accuracy of the scheme is not of primary importance. Note also that it is Eqs. (12) to (14) that are actually used in most applications to estimate the truncation errors.

For the second derivatives, $x_{\xi\xi}$ can be expressed as

$$\begin{aligned} x_{\xi\xi} &= \frac{(x_{i+1,j} - x_{i,j}) - (x_{i,j} - x_{i-1,j})}{(\Delta\xi)^2} \\ &= a\cos\gamma - ar_1\cos(\gamma + \Delta\gamma) \\ &= a\cos\gamma(1 - r_1\cos\Delta\gamma) + ar_1\sin\gamma\sin\Delta\gamma \end{aligned}$$

and, similarly,

$$\begin{aligned} x_{\eta\eta} &= b\sin\beta(1 - r_2\cos\Delta\beta) + br_2\cos\beta\sin\Delta\beta \\ y_{\xi\xi} &= a\sin\gamma(1 - r_1\cos\Delta\gamma) + ar_1\cos\gamma\sin\Delta\gamma \\ y_{\eta\eta} &= b\cos\beta(1 - r_2\cos\Delta\beta) + br_2\sin\beta\sin\Delta\beta. \end{aligned} \tag{16}$$

Let

$$\begin{aligned} R_{\xi C2} &= 1 - r_1\cos\Delta\gamma \\ R_{\xi S2} &= r_1\sin\Delta\gamma \\ R_{\eta C2} &= 1 - r_2\cos\Delta\beta \\ R_{\eta S2} &= r_2\sin\Delta\beta. \end{aligned}$$

Equation (16) can then be written as

$$\begin{aligned} x_{\xi\xi} &= aR_{\xi C2}\cos\gamma + aR_{\xi S2}\sin\gamma \\ x_{\eta\eta} &= bR_{\eta C2}\sin\beta - bR_{\eta S2}\cos\beta \\ y_{\xi\xi} &= aR_{\xi C2}\sin\gamma - aR_{\xi S2}\cos\gamma \\ y_{\eta\eta} &= bR_{\eta C2}\cos\beta + bR_{\eta S2}\sin\beta. \end{aligned} \tag{17}$$

One may call parameters R's the grid smoothness parameters, which are functions of grid size ratios and changes of gridline angles. They can also be considered as measures of grid skewness and deviation from uniformity. Note that in a parallel uniform grid system, these grid smoothness parameters assume the value of zero. On the other hand, with a highly skewed and nonuniform grid, these parameters can have large values.

For the third derivatives,

$$\begin{aligned} x_{\xi\xi\xi} &= \frac{a}{2}(R_{\xi C3}\cos\gamma - R_{\xi S3}\sin\gamma) \\ y_{\xi\xi\xi} &= \frac{a}{2}(R_{\xi C3}\sin\gamma + R_{\xi S3}\cos\gamma) \\ x_{\eta\eta\eta} &= \frac{b}{2}(R_{\eta C3}\sin\beta + R_{\eta S3}\cos\beta) \\ y_{\eta\eta\eta} &= \frac{b}{2}(R_{\eta C3}\cos\beta - R_{\eta S3}\sin\beta), \end{aligned} \tag{18}$$

where

$$\begin{aligned} R_{\xi C3} &= r_{11}\cos\Delta\gamma_{11} + r_{12}\cos\Delta\gamma_{12} - r_1\cos\Delta\gamma - 1 \\ R_{\xi S3} &= r_{11}\sin\Delta\gamma_{11} + r_{12}\sin\Delta\gamma_{12} - r_1\sin\Delta\gamma \\ R_{\eta C3} &= r_{21}\cos\Delta\beta_{21} + r_{22}\cos\Delta\beta_{22} - r_2\cos\Delta\beta - 1 \\ R_{\eta S3} &= r_{21}\sin\Delta\beta_{21} + r_{22}\sin\Delta\beta_{22} - r_2\sin\Delta\beta. \end{aligned}$$

Again, these grid smoothness parameters reduce to zero in a parallel uniform grid system. Furthermore, contravariant velocities can be written as

$$\begin{aligned} \bar{U} &\equiv uy_\eta - vx_\eta = Vb\sin(\gamma+\theta-\alpha) \\ \bar{V} &\equiv vx_\xi - uy_\xi = Va\sin(\alpha-\gamma), \end{aligned} \tag{19}$$

where V represents the total velocity. It is observed that $\rho\bar{U}$ represents the flow rate normal to the η line and $\rho\bar{V}$ represents the flow rate normal to the ξ line; note that $\rho\bar{U}$ and $\rho\bar{V}$ make an angle of θ. Expressions (15) to (18) can be substituted into Eqs. (12) to (14) to yield

$$\begin{aligned} T_{E1} = \frac{\rho V}{4\sin\theta}\{&\sin(\gamma+\theta-\alpha)[(\cos\gamma f_x + \sin\gamma f_y)R_{\xi C3} \\ &+ (-\sin\gamma f_x + \cos\gamma f_y)R_{\xi S3}] + \sin(\alpha-\gamma) \\ &\times[(\cos(\gamma+\theta)f_x + \sin(\gamma+\theta)f_y)R_{\eta C3} \\ &+ (\sin(\gamma+\theta)f_x - \cos(\gamma+\theta)f_y)R_{\eta S3}]\} \end{aligned} \tag{20}$$

$$\begin{aligned} T_{E2} = \frac{\rho V}{\sin\theta}\{&a\sin(\gamma+\theta-\alpha)[(\cos^2\gamma f_{xx} + 2\cos\gamma\sin\gamma f_{xy} \\ &+ \sin^2\gamma f_{yy})R_{\xi C2} \\ &+ (\sin\gamma\cos\gamma f_{xx} + (\sin^2\gamma - \cos^2\gamma)f_{xy} \\ &- \sin\gamma\cos\gamma f_{yy})R_{\xi S2}] + b\sin(\alpha-\gamma) \\ &\times[(\cos^2(\gamma+\theta)f_{xx} + 2\cos(\theta+\gamma)\sin(\theta+\gamma)f_{xy} \\ &+ \sin^2(\theta+\gamma)f_{yy})R_{\eta C2} + (-\sin(\theta+\gamma)\cos(\theta+\gamma)f_{xx} \\ &+ (\cos^2(\theta+\gamma) - \sin^2(\theta+\gamma))f_{xy} \\ &+ \cos(\theta+\gamma)\sin(\theta+\gamma)f_{yy})R_{\eta S2}]\} \end{aligned} \tag{21}$$

$$\begin{aligned} T_{E3} = \frac{\rho V}{3\sin\theta}\{&a^2\sin(\gamma+\theta-\alpha)(\cos^3\gamma f_{xxx} \\ &+ 3\cos^2\gamma\sin\gamma f_{xxy} + 3\cos\gamma\sin^2\gamma f_{xyy} + \sin^3\gamma f_{yyy}) \\ &+ b^2\sin(\alpha-\gamma)[\cos^3(\theta+\gamma)f_{xxx} \\ &+ 3\cos^2(\theta+\gamma)\sin(\theta+\gamma)f_{xxy} \\ &+ 3\cos(\theta+\gamma)\sin^2(\theta+\gamma)f_{xyy} \\ &+ \sin^3(\theta+\gamma)f_{yyy}]\}. \end{aligned} \tag{22}$$

Table I lists the common and different factors among T_{E1}, T_{E2}, and T_{E3}.

Observing the general Eqs. (20) to (22), a few remarks are useful. First of all, T_{E1} does not contain the grid size a or b and therefore is of zero-order accuracy. This implies that if T_{E1} is dominant, grid refinement will not ensure error reduction. Second, T_{E1} and T_{E2} will disappear if a uniform parallel grid is employed as can be seen in Eqs. (23) and (24) below. Note also that T_{E1} and T_{E2} contain the grid smoothness parameters, but expression T_{E3} does not, and therefore grid skewness ($\Delta\beta$, $\Delta\gamma$, $\Delta\beta_{ij}$, $\Delta\gamma_{ij}$) and grid uniformity (r_i, r_{ij}) do not affect T_{E3}. On the other hand, grid uniformity may play a very important role in T_{E1} and T_{E2} if the values of r_i, r_{ij} are much larger or smaller than unity, since they may dominate the grid smoothness factors which are the multipliers in the expressions. This is consistent with the observation of Castro and Jones [2]. They pointed out that there will be significant zero-order errors unless the mesh expansion ratios are close to unity. Third, when the total velocity vector aligns with one of the gridlines, that is, $\alpha = \gamma$

TABLE I

Common and Different Factors in T_{E1}, T_{E2}, T_{E3}

	Common	Different
T_{E1}	$\rho, V, \gamma, \theta, \alpha, \beta$	$r_i, r_{ij}, \Delta\beta, \Delta\beta_{ij}, \Delta\gamma, \Delta\gamma_{ij}, f_{(1)}$
T_{E2}	$\rho, V, \gamma, \theta, \alpha, \beta$	$a, b, r_i, \Delta\beta, \Delta\gamma, f_{(2)}$
T_{E3}	$\rho, V, \gamma, \theta, \alpha, \beta$	$a^2, b^2, f_{(3)}$

or $\alpha = \theta + \gamma$, half of the terms in Eqs. (20) to (22) can be dropped, and this may significantly reduce the truncation errors. Finally, the individual grid angles $\alpha, \beta, \gamma, \theta$ may or may not be important, since truncations errors also depend on the combination of these angles. These combined angles represent the gridline angle relative to the x-axis $(\gamma + \theta)$ and the angles between the gridlines and the total velocity vector $(\gamma + \theta - \alpha, \alpha - \gamma)$. To construct an optimal grid angle, the interactions between grid distribution and flow field (representing by various function derivatives $f_{(i)}$'s) should be taken into account. Unfortunately, this is very difficult in practice. However, it is obvious that grid orthogonality does not guarantee that the truncation error can be minimized. The observations above imply that both grid size reduction and grid quality improvement can cause error reduction in general.

It is possible to further simplify Eqs. (20) to (22) with a special grid arrangement. For example, consider the grids with parallel and straight grid lines, that is, $\Delta\gamma = \Delta\gamma_{11} = \Delta\gamma_{12} = \Delta\beta = \Delta\beta_{21} = \Delta\beta_{22} = 0$, so that

$$T_{E1} = \frac{\rho V}{4 \sin\theta} \{\sin(\gamma + \theta - \alpha)(\cos\gamma f_x + \sin\gamma f_y) \times (r_{11} + r_{12} - r_1 - 1) + \sin(\alpha - \gamma)[\cos(\gamma + \theta) f_x + \sin(\gamma + \theta) f_y](r_{21} + r_{22} - r_2 - 1)\} \quad (23)$$

$$T_{E2} = \frac{\rho V}{\sin\theta} \{a \sin(\gamma + \theta - \alpha)(\cos^2\gamma f_{xx} + 2\cos\gamma \sin\gamma f_{xy} + \sin^2\gamma f_{yy})(1 - r_1) + b \sin(\alpha - \gamma)[\cos^2(\gamma + \theta) f_{xx} + 2\cos(\theta + \gamma)\sin(\theta + \gamma) f_{xy} + \sin^2(\theta + \gamma) f_{yy}](1 - r_2)\} \quad (24)$$

$$T_{E3} = \frac{\rho V}{3 \sin\theta} \{a^2 \sin(\gamma + \theta - \alpha) \times (\cos^3\gamma f_{xxx} + 3\cos^2\gamma \sin\gamma f_{xxy} + 3\cos\gamma \sin^2\gamma f_{xyy} + \sin^3\gamma f_{yyy}) + b^2 \sin(\alpha - \gamma) \times [\cos^3(\theta + \gamma) f_{xxx} + 3\cos^2(\theta + \gamma)\sin(\theta + \gamma) f_{xxy} + 3\cos(\theta + \gamma)\sin^2(\theta + \gamma) f_{xyy} + \sin^3(\theta + \gamma) f_{yyy}]\}. \quad (25)$$

Note that T_{E3}, which is free from grid smoothness parameters, is not altered by this simplification. From the above equations, it is clear that the truncation error depends upon the grid sizes a and b, the combined angles such as $\gamma + \theta - \alpha$, $\gamma + \theta$, $\alpha - \gamma$ and grid size ratios r_1's, r_2's. It should be pointed out that in the case of large r's (and/or large grid smoothness parameters R's), large errors may result. It is also worth noting that if a small geometric expansion ratio $\varepsilon \ll 1$ (i.e., $r_{11} = 1 + \varepsilon$, $r_1 = 1/1 + \varepsilon$, etc.) is employed, as is common in grid distribution, then from Eqs. (23) and (24), it is seen that $T_{E1} = O(\varepsilon^2)$ and $T_{E2} = O(\varepsilon)$.

If other second-order differencing schemes are employed in Eq. (1), the only difference in expressions (4) to (6) is the leading constants. For example, with the second-order central scheme, the leading constants in Eqs. (4), (5), and (6) become $-\frac{1}{6}$, $-\frac{1}{2}$ and $-\frac{1}{6}$, respectively. Therefore, the truncation error formula obtained above can still be used as a good indicator for the truncation error distribution in a more general sense. In the next section test cases are used to demonstrate some characteristics of the expressions. In these problems, second-order upwind and second-order central schemes are employed for the convection and diffusion terms, respectively.

TEST PROBLEMS AND DISCUSSION

To assess the usefulness of the derived formula, a fully developed channel flow with exact solution is employed. The Reynolds number based on the inlet velocity and height is 200. In this test case, the computed truncation errors using Eqs. (12) to (14) are compared to those estimated by the exact solution. The skew grid is arbitrarily designed as shown in Fig. 2. The grid number is 10×49. The contours shown in Fig. 3a are obtained by taking the difference between the computed value and the exact value of the convection terms, that is,

$$\mathscr{L}f - L_h f_h,$$

where $\mathscr{L}$ and L_h are the differential and difference operators for the convection terms, f, f_h are the exact solution and the computed solution based on a 10×49 grid, respectively. Figure 3b shows the truncation error distribution for the u

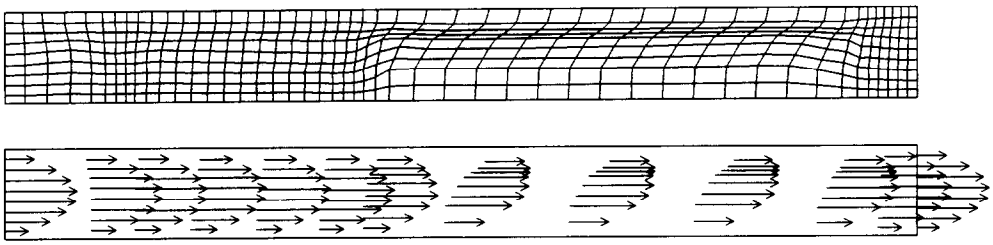

FIG. 2. Skew grid arrangement for the fully developed channel flow.

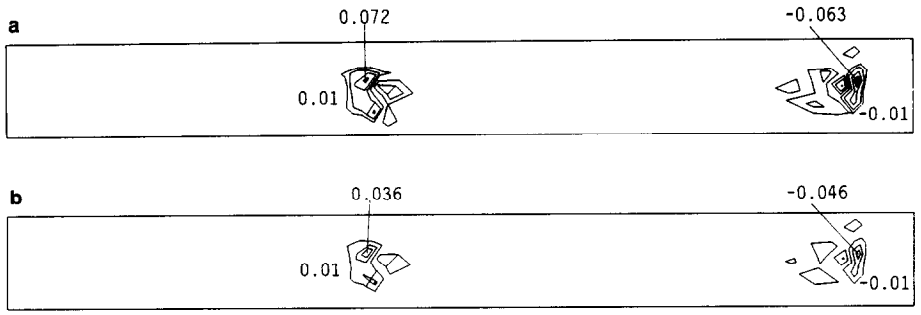

FIG. 3. Truncation error contours for convection terms of U momentum equation.

momentum equation calculated using Eqs. (12) to (14). The resemblance between the two plots is clearly illustrated. The errors are concentrated in the regions where the grid changes abruptly. This observation can be justified by using Eqs. (12) to (14). In these equations, since the flow is fully developed, $\bar{U} \gg \bar{V}$ in most regions where the ξ gridline is horizontal. Moreover, all the f derivatives with respect to x can be dropped, and the remaining terms (with $y_{\xi\xi\xi}$, $y_{\xi\xi}$, etc.) will then be large when the grid changes suddenly.

Equations (20) to (22) are in general form for the present test cases; careful observation of these equations reveals that it is difficult to separate the effect of each factor. However, the following two cases with a specially designed grid may be used to demonstrate, first of all, the effect of gridline angle (grid orthogonality) on the truncation error and, second, the usefulness of the derived formula in estimating the truncation error distribution. The first test case for these purposes is a laminar channel flow with two different velocity layers. To show the effect of gridline angle θ, zigzag grid lines are employed to construct the grid. Although this grid arrangement is not of practical interest, it may simplify the derived formula and single out the role of the angle θ in truncation errors. The next problem is a laminar backward-facing step flow with a parabolic inlet velocity. Again, zigzag grids are used to show the role of the angle θ in truncation errors. For both of the above two test cases, since exact

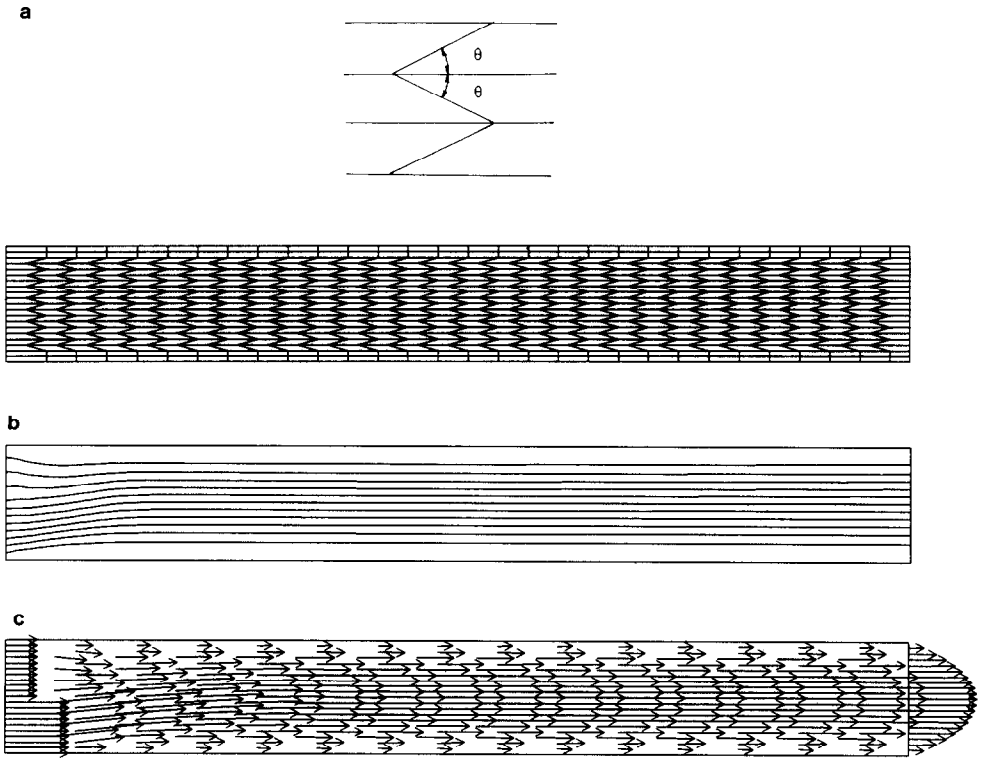

FIG. 4. Grid arrangement, streamlines and velocity distribution of the channel flow with two different velocity layers: (a) grid arrangement; (b) streamlines; (c) velocity vectors.

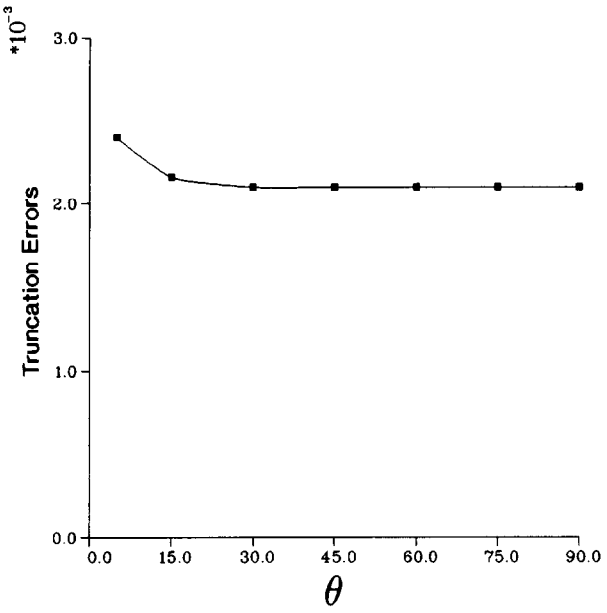

FIG. 5. The effect of θ angle on overall truncation errors for convection terms of u momentum equation (two-layer flow).

solution is not available, a uniform fine grid solution is used as a reference for comparison.

For the first test flow problem, its grid arrangement and streamlines are shown in Fig. 4. In this problem, streamlines are parallel to the ξ lines except near the inlet region. Since the grid is uniform along the ξ lines, $r_1 = r_2 = r_{ij} = 1$, $\alpha \approx 0$, $\gamma = 0$, $\beta = 90° - \theta$, $\Delta\gamma = \Delta\gamma_{11} = \Delta\gamma_{12} = 0$, $\Delta\beta_{22} = 0$, $\Delta\beta = \Delta\beta_{21} = 180° + 2\theta$. Consequently, from Eqs. (20) to (22), T_{E1} and T_{E2} can be eliminated and T_{E3} becomes

$$T_{E3} \approx \frac{\rho V}{3} a^2 f_{xxx}. \tag{26}$$

Obviously, Eq. (26) is independent of θ. Numerically, a reference solution of this flow problem is obtained by using a uniform grid of 101 × 101. A zigzag grid solution of 31 × 21 is then used to display the effect of θ on truncation errors. In Fig. 5 it can be seen that change in θ does not change the overall truncation errors of convection terms over most of the range unless θ is very small. The overall convection term error in Fig. 5 is estimated numerically by summing the difference of the values of the fine grid (101 × 101) convection terms and the coarse grid (31 × 21) convection terms at each grid point and then dividing by the total number of grids N; that is,

$$\frac{1}{N} \sum_{i=1}^{N} |(Lf)_{101 \times 101} - (Lf)_{31 \times 21}|_i,$$

where L is the difference operator for the convection terms as mentioned above. The computed result is consistent with expression (26). This implies that similar accuracy can be obtained whether one uses small θ grids or orthogonal grids. Although not shown here, the solution error (relative to the reference solution) has similar behavior.

Specifications and computed streamlines of the second test problem are shown in Fig. 6. A backward-facing step flow with a parabolic inlet velocity and average Reynolds number of 800 is used. The reference solution of this problem is again obtained by using a uniform fine grid of 101 × 101. The zigzag grid in Fig. 4 is also used in this problem. In this case, all the simplifications made in the last test case are the same except that α is no longer zero, and therefore, Eq. (20) is eliminated again and Eqs. (21) and (22) assume the forms of

$$T_{E2} = \frac{\rho V b}{\sin\theta} \sin\alpha \cos\theta (2\cos\theta f_{xx} + 2\sin\theta f_{xy})$$

$$T_{E3} = \frac{\rho V}{3\sin\theta} [a^2 \sin(\theta - \alpha) f_{xxx} + b^2 \sin\alpha (\cos^3\theta f_{xxx} + 3\cos^2\theta \sin\theta f_{xxy} + 3\cos\theta \sin^2\theta f_{xyy} + \sin^3\theta f_{yyy})]. \tag{27}$$

In this particular case, some velocity derivatives are much smaller than others, and therefore those derivatives are neglected. Numerically, it can be shown that $|f_{yy}| \gg |f_{xy}| > |f_{xx}|$ and $|f_{yyy}| \gg |f_{xxx}|, |f_{xyy}|, |f_{xxy}|$ in most of the region. To provide accurate values so that the following simplified formula can stand, all the f derivatives are

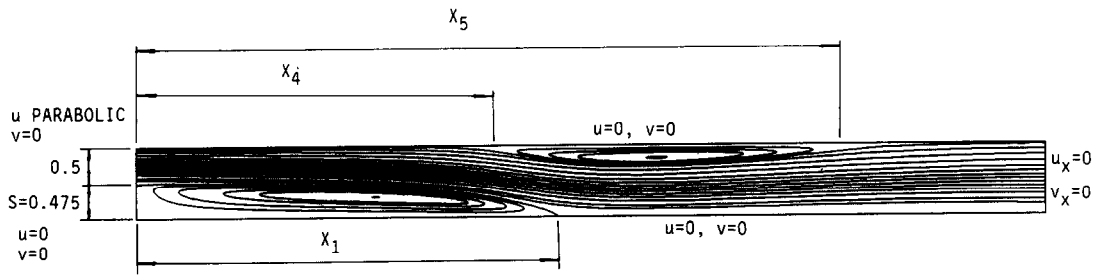

FIG. 6. The backward-facing step flow.

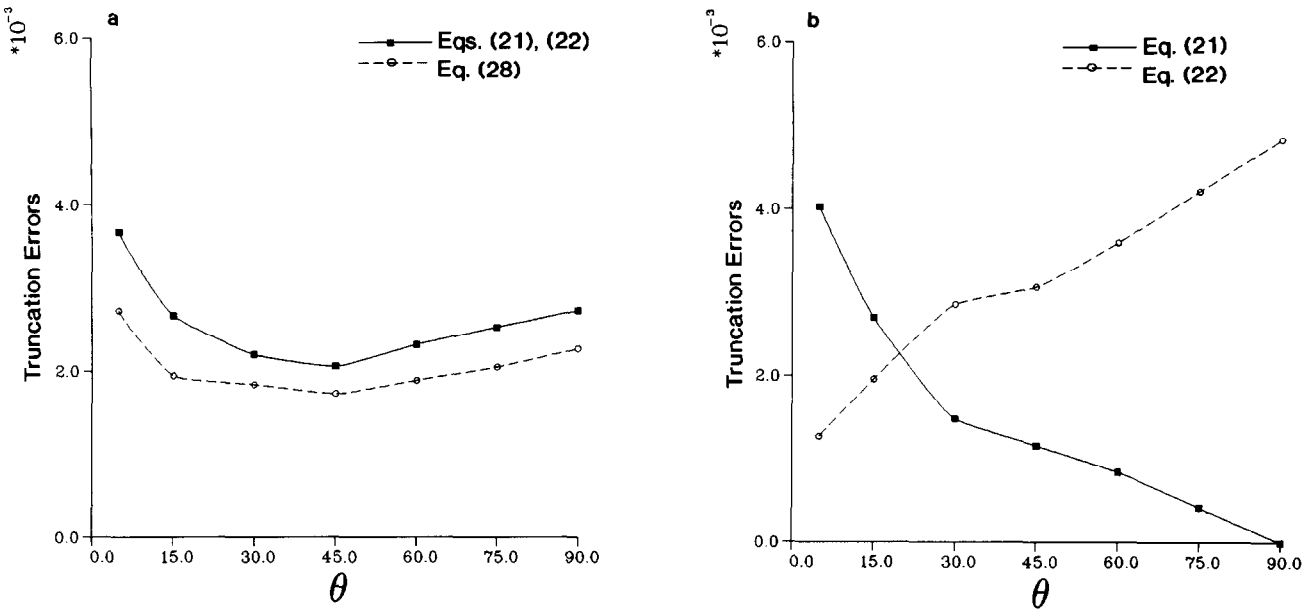

FIG. 7. The effect of θ angle on truncation errors for convection terms of u momentum equation (step flow): (a) truncation errors obtained by Eqs. (21), (22), and (28), respectively; (b) effect of θ angle on T_{E2} and T_{E3}.

calculated based on the fine grid solution and the mixed partial derivatives are calculated by a method which is accurate to the second order for both Δx and Δy [6]. Therefore, the truncation error can be approximated as

$$\begin{aligned} T_E &= T_{E2} + T_{E3} + \text{Higher Order Terms} \\ &\approx 2\rho Vb \sin\alpha \cos\theta f_{xy} + \frac{\rho Vb^2}{3} \sin^2\theta \sin\alpha f_{yyy} \\ &\quad + \text{Higher Order Terms} \\ &\approx \rho Vb \sin\alpha \left(2\cos\theta f_{xy} + \frac{b}{3}\sin^2\theta f_{yyy}\right) \\ &\quad + \text{Higher Order Terms.} \end{aligned} \tag{28}$$

The overall truncation errors of convection terms computed by Eqs. (21), (22), and (28), respectively, are plotted in Fig. 7a. Equation (28) is a fair approximation to the combination of Eqs. (21) and (22). Obviously, Eq. (28) indicates that $\theta = 90°$ does not yield the minimum T_E and the optimal θ is strongly influenced by the derivatives of flow properties such as f_{xy} and f_{yyy}. In Fig. 7b, T_{E2} is seen to decrease as θ increases. At $\theta = 90°$, T_{E2} vanishes, as expected for an orthogonal grid. On the other hand, T_{E3} increases with θ. Note that T_{E1} is vanishingly small in all cases of this problem, as it should be theoretically. The truncation errors estimated numerically by the same method used in Fig. 5 are shown in Fig. 8. Similar trends are observed in Fig. 7a and Fig. 8. This result further confirms the usefulness of the derived formula. In Fig. 9, three θ angles are chosen to demonstrate the distribution of errors. This figure again shows that an orthogonal grid does not guarantee best results. Most errors occur in the shear layer region. Figure 10 depicts the truncation error contours of the u momentum equation estimated numerically using the same method used in Fig. 3a. A similar effect of θ on the error distribution is observed. The truncation error formula is shown to be a fairly good error indicator. On the prediction of the reattachment lengths defined in Fig. 6, Fig. 11 again shows a similar trend in the effect of θ on the solution, and the case with $\theta = 90°$ is not the best one.

Two things are observed from the results of these test problems. First of all, the expressions for the truncation

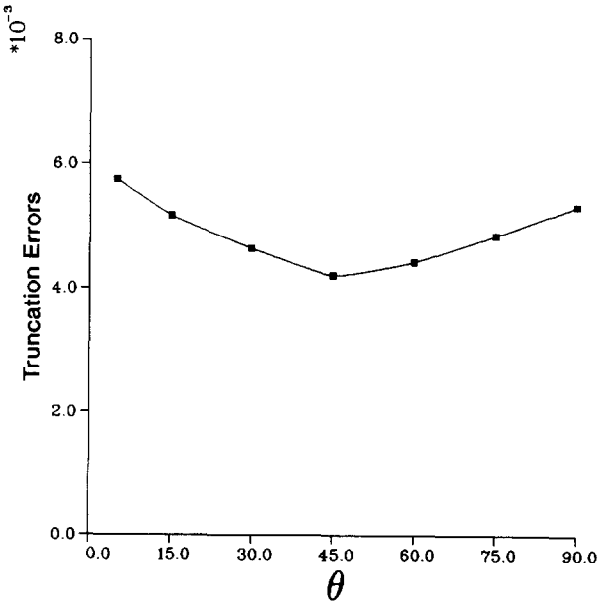

FIG. 8. The effect of θ angle on overall truncation errors for convection terms of u momentum equation (step flow).

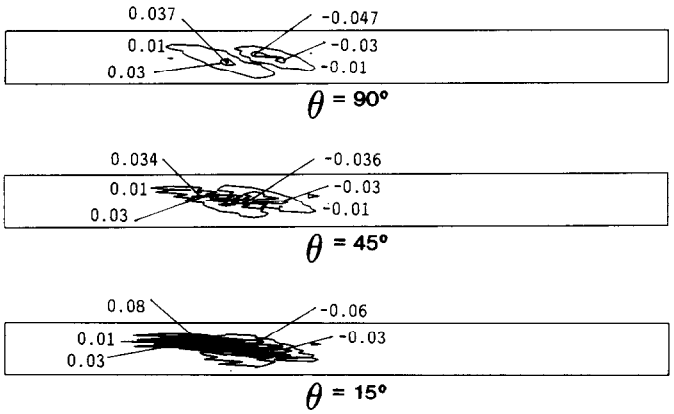

FIG. 9. Truncation error contours for convection terms of u momentum equation at different θ angle, estimated by the formula.

errors of the convection terms closely describe the actual numerical errors of the flow problem. Second, the most accurate solution does not take place at $\theta = 90°$. A similar observation was pointed out by Shyy and Braaten [7]. They investigated the effect of grid line angle θ on the accuracy of the numerical solution. A series of two-dimensional, fully developed flow calculations were performed for a square duct. Four different grids corresponding to grid orientations of 0°, 15°, 30°, and 45° about the reference Cartesian coordinates were used. As the angle of rotation increased, the grid changes from an orthogonal uniform rectangular grid to one with increasing skewness and nonorthogonality. They found that for the same number of grid points, the highly skewed grid gave a more accurate center point location and a 151×151 uniform grid was required in their case to achieve the same accuracy as the 51×51 skewed grid with 45° rotation.

As demonstrated in Eqs. (20) to (22), it is clear that to minimize the truncation errors one should reduce the grid size as well as improve the grid quality (grid skewness and the grid smoothness). Reducing grid size remains the most straightforward means in reducing the higher order errors,

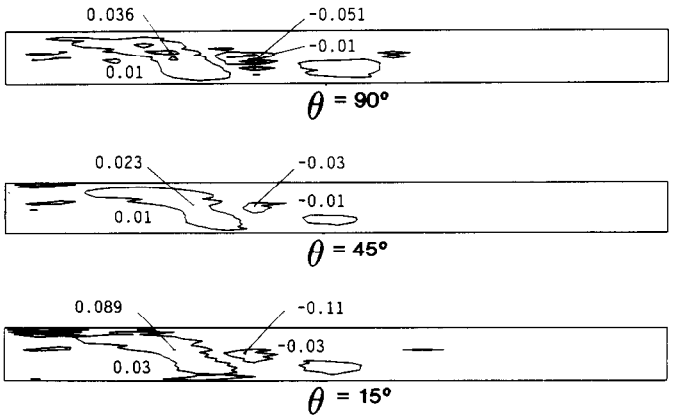

FIG. 10. Truncation error contours for convection terms of u momentum equation at different θ angle, estimated by using reference solution.

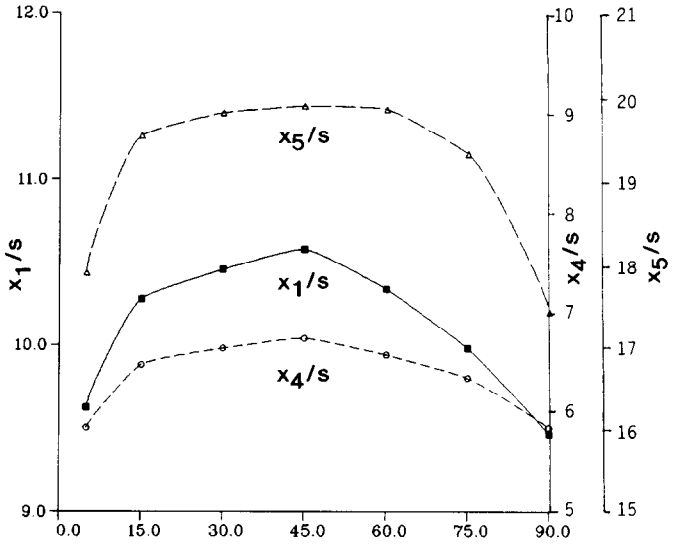

FIG. 11. The effect of θ angle on predicted reattachment lengths of the backward facing step.

however, this should be subject to the limitations of computer resources; therefore grid size reduction should be limited to those regions which need higher resolution. Better grid quality also helps in reducing errors. An optimal grid arrangement is very much flow field dependent and is generally difficult to achieve as mentioned before. According to Eqs. (20) to (22), when the total velocity aligns with one of the grid lines (e.g., $\alpha = \gamma + \theta$), many terms in the expressions can be dropped, and this may significantly reduce the truncation errors. Therefore, to better resolve flow problems, it seems natural to align grid lines according to the flow stream and cluster grids in the regions, where local truncation errors are large, to reduce both the grid sizes and the truncation errors. Consequently, the adaptive grid method appears to be a good approach. As an application, in the final test case the truncation error formula is applied to estimate errors of an adaptive solution.

The equidistribution scheme of grid adaption employed by Dwyer *et al.* [8] is modified [9] and used in the present problem to construct the adaptive grid. The weight function in the x direction at the ith grid assumes the form

$$W_i = 1 + (\phi_x)_i + \sum_{k=1, k\neq i}^{n} (\phi_x)_k \cdot C_t \cdot \exp(-|i-k|), \quad (29)$$

where C_t is an arbitrary constant for the control of the coupling of the weight functions among neighboring grids. The third term on the right-hand side of Eq. (29) is to account for the influence of the property gradients of the neighboring grids in grid adaption, and this influence is assumed to decay exponentially. In the regions of large gradient change, this term may ease the sudden change of the grid size. This modified method was shown [9] to

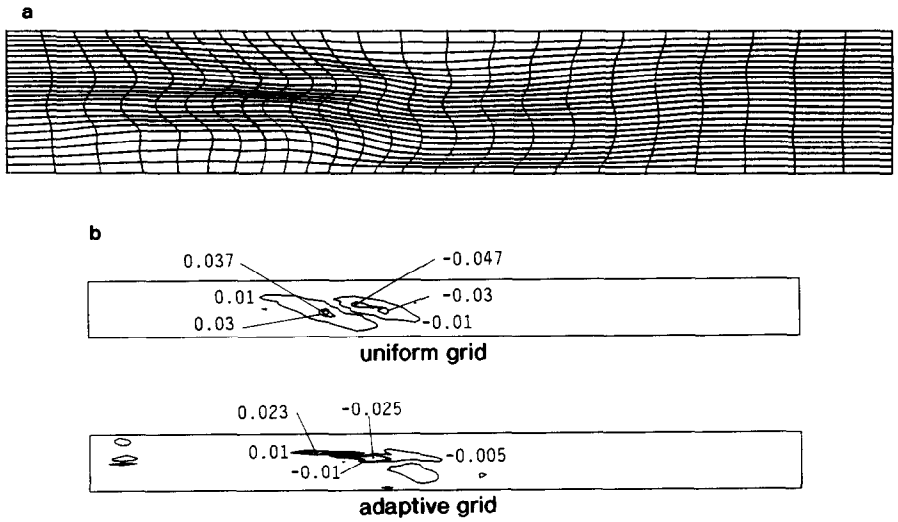

FIG. 12. (a) Adaptive grid for the backward facing step flow. (b) The truncation error contours for the uniform and adaptive grid solutions.

improve both grid quality and solution accuracy as compared to the original one.

The adaptive grid so constructed is shown in Fig. 12. Also shown in the figure are the truncation error contours obtained on a uniform grid and on an adaptive grid. The truncation errors are computed using Eqs. (12) to (14). The application of adaptive gridding reduces the maximum truncation error and the overall truncation errors as well.

Theoretically, in performing grid adaption, the grid should be fine at points where the local truncation error is large and not at points where the flow property gradient is large, as pointed out by Hedstrom and Rodrique [10]. However, in practice, direct evaluation of local truncation error is not straightforward. Error estimates are often obtained by the method such as the Richardson extrapolation, which requires calculation of the flow field with two different mesh sizes. The difference between the solutions at the same grid point is then used as an estimate of the error [11]. The computational overhead of this method is not trivial. The truncation error formula derived in this study provides a useful indicator of local truncation error. Further use of the formula in adaptive grid methods is currently being studied by the authors [12].

CONCLUSIONS

From the expressions for truncation error and the results of test problems, some observations can be summarized. First, should T_{E1} appear in the expressions, it cannot be reduced by decreasing the grid size, since T_{E1} is independent of grid size. This implies that if T_{E1} is dominant in the computation, grid refinement does not necessarily ensure the error reduction. For a curvilinear coordinate system, T_{E2} is in general the leading truncation error term and is of the first order of accuracy. T_{E2} can be eliminated if a uniform parallel grid is employed; grid orthogonality is not a must to eliminate T_{E2}. It is also noted that grid uniformity and grid skewness have no effect on T_{E3}. Grid skewness lowers the order of accuracy through T_{E1} and T_{E2}. Second, if the grids are so distributed that the gridlines align with the total velocity vector or streamline, many terms in T_{E2} and T_{E3} can be dropped, and this in general reduces the truncation error of the convection terms. Third, the use of an orthogonal grid in general does not guarantee truncation error reduction, and this is seen in the results of both test problems as well as in the simplified equations (26) and (28). The remarks made by Thompson *et al.* [5] on the angle θ should not be misinterpreted. An optimal grid arrangement is in general strongly dependent upon the flow field. Therefore, to optimize the truncation errors, use of grid adaption based on the flow field is suggested.

The formula derived in the present study clearly demonstrates important factors which affect the truncation errors of two-dimensional convective terms. To reduce truncation errors, this formula reveals that the following factors are relevant: grid size, grid size ratio, angle between the gridlines, angle of velocity vector relative to the gridline, grid uniformity and skewness, and derivatives of flow properties. From the truncation error expressions, one may find that it is impossible to determine the best grid exactly, due to the strong connection between the flow field and the grid itself. Nevertheless, in constructing a curvilinear grid, one should keep the grid as smooth as possible to reduce T_{E1}, T_{E2}, and one should reduce grid size where needed to reduce T_{E2}, T_{E3}, and higher order error terms. With limited grids, adaptive gridding provides a partial solution to grid optimization. The present formula also provides a useful indicator of truncation error distribution.

REFERENCES

1. E. K. de Rivas, *J. Comput. Phys.* **10**, 202 (1972).
2. I. P. Castro and J. M. Jones, *Int. J. Numer. Methods* **7**, 793 (1987).
3. C. K. Forester, AIAA Paper 81-0002, 1981 (unpublished).
4. J. F. Thompson and C. W. Mastin, "Order of Difference Expressions in Curvilinear Coordinate Systems," ASME, FED **5**, p. 17, 1983.
5. J. F. Thompson, Z. U. A. Warsi, and C. W. Mastin, *Numerical Grid Generation* (North-Holland, New York, 1982), Chap. 5.
6. D. A. Anderson, J. C. Tannehill, and R. H. Pletcher, *Computational Fluid Mechanics and Heat Transfer* (McGraw–Hill, New York, 1984), Chap. 3.
7. W. Shyy and M. E. Braaten, "Applications of A Generalized Pressure Correction Algorithm for Flows in Complicated Geometries," in *Advances and Applications in Computational Fluid Dynamics*, edited by O. Baysal, ASME, FED **66**, 1989.
8. H. A. Dwyer, R. J. Kee, and B. R. Sanders, *AIAA J.* **18**, No. 10, 1205 (1980).
9. D. Lee and Y. M. Tsuei, *Int. J. Numer. Methods*, in press.
10. G. W. Hedstrom and G. H. Rodrique, in *Multigrid Method*, Lecture Notes in Math., Vol. 960 (Springer-Verlag, Berlin, 1982), p. 474.
11. S. C. Caruso, J. H. Ferziger, and J. Oliger, AIAA Paper 86-0498, 1986 (unpublished).
12. D. Lee and Y. M. Tsuei, *J. Comput. Phys.*, submitted.